Open Ceramics 5 (2021) 100056

Contents lists available at ScienceDirect

Open Ceramics

journal homepage: www.editorialmanager.com/oceram

Combination of PIP and LSI processes for SiC/SiC ceramic matrix composites

Fabia Süß [a,*], Tobias Schneider [b], Martin Frieß [a], Raouf Jemmali [a], Felix Vogel [a], Linda Klopsch [a], Dietmar Koch [b]

[a] German Aerospace Center (DLR), Institute of Structures and Design, Pfaffenwaldring 38-40, 70569 Stuttgart, Germany
[b] University of Augsburg, Institute of Materials Resource Management, Am Technologiezentrum 5, 86159 Augsburg, Germany

ARTICLE INFO

Keywords:
SiC/SiC ceramic matrix composites
PIP and LSI processes
CVD fiber coating

ABSTRACT

Silicon carbide fiber-reinforced silicon carbide matrix composites (SiC/SiC CMCs) are promising candidates for hot gas components in jet engines. Three common manufacturing routes are chemical vapor infiltration, reactive melt infiltration (RMI) and polymer infiltration and pyrolysis (PIP). A combination of the processes seems attractive: the remaining porosity after PIP process can be closed by subsequent siliconization, resulting in a dense material. This work describes a new approach of a combined PIP and RMI process. SiC/SiC CMCs were manufactured by PIP process using Hi-Nicalon Type S fibers. An additional RMI was carried out after a reduced number of PIP cycles. Microstructure was examined via µCT, SEM and EDS. Bending strength was determined to 433 MPa; strain to failure was 0.60%. The overall processing time was reduced by 55% compared to standard PIP route. The hybrid material contained 70% less unreacted carbon than material produced by LSI process alone.

1. Introduction

Silicon carbide fiber-reinforced silicon carbide matrix composites (SiC/SiC CMCs) are promising materials for the application in aircraft turbine engines. Compared to their metallic counterparts, they have a higher temperature resistance and lower density, which enables to increase the operating temperature and reduce the required cooling air. Lower fuel consumption and an overall higher efficiency of jet engines can be achieved [1]. This also leads to a reduction of emissions, which is an important goal in EUs strategy paper Flightpath 2050 [2].

In literature, three common processing routes for SiC/SiC CMCs are described in detail: chemical vapor infiltration (CVI), polymer infiltration and pyrolysis (PIP), and reactive melt infiltration (RMI) [3]. CVI process is mainly used for nuclear applications such as fuel claddings due to the radiation resistant properties of the material [4–6]. The most famous representative of melt infiltrated (MI) SiC/SiC is General Electric's HiPerComp material. SiC/SiC composite high-pressure turbine shrouds have been commercially introduced in the LEAP engine in 2016. For the new GE9X engine five CMC components are announced including combustor liners, shrouds and nozzles [7–9]. In PIP process polymer derived amorphous SiC, SiCO or SiCN ceramics are introduced into a fiber preform. As precursors preceramic organosilicon polymers such as polycarbosilanes, polysiloxanes or polysilazanes are used [10–13].

However, literature provides little information on hybrid manufacturing processes that use a combination of more than one route, especially not for PIP and RMI. For the manufacturing of SiC/SiC CMCs, Licciulli et al. and Ortona et al. used CVI followed by the infiltration and pyrolysis of polycarbosilanes with an optional SiC nanopowder as filler [14,15]. Nannetti et al. used a similar process but performed a SiC powder slurry infiltration between CVI and PIP process to fill the large interbundle porosity [16]. However, CVI processes applied in both techniques were mainly used to apply a debonding layer onto fibers to avoid brittle fracture and play a minor role in matrix construction. Suzuki et al. used a pulsed CVI process as a finishing process after slurry infiltration and PIP to manufacture C/SiC CMCs. They found that the last CVI step is beneficial for bending strength [17]. Schoenfeld and Klemm used a winding technique and impregnated the SiC fiber roving with a slurry which contains SiC powder and sintering aids. After several PIP cycles with polysilazanes, they used an additional sintering step to achieve crack healing and a homogeneous matrix. They obtained damage tolerant composites with a bending strength level of 500 MPa [18].

This work describes the polymer infiltration and pyrolysis process followed by a liquid silicon infiltration (LSI) step for the first time. So far,

* Corresponding author.
E-mail address: fabia.suess@dlr.de (F. Süß).

https://doi.org/10.1016/j.oceram.2021.100056
Received 30 October 2020; Received in revised form 18 December 2020; Accepted 4 January 2021
Available online 7 January 2021

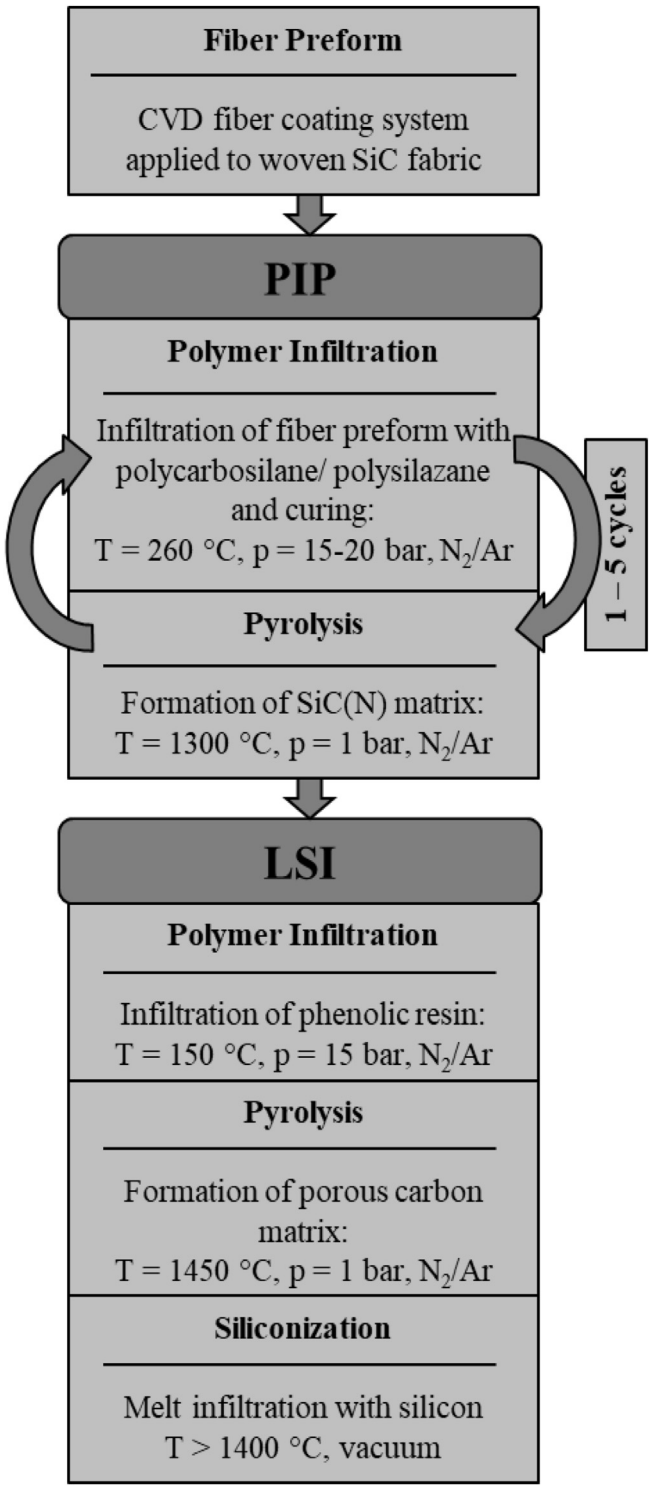

Fig. 1. Scheme of the hybrid manufacturing process consisting of polymer infiltration and pyrolysis (PIP) and liquid silicon infiltration (LSI).

this combination could not be found in literature. At German Aerospace Center (DLR), both routes PIP and LSI are used for the manufacturing of SiC/SiC CMC. Each individual process was investigated in detail, but till now, they have never been combined. The method of PIP and the resulting microstructure as well as mechanical properties were described by Mainzer et al. [13,19,20]. The manufacturing of SiC/SiC via liquid silicon infiltration is assigned to RMI procedures. The process steps of LSI and the fiber coating system which protects the fibers from the aggressive silicon melt were described in detail in earlier works [21].

Both processing routes have advantages and disadvantages. PIP material shows very good fracture toughness even without any additional fiber coating. But due to the nature of the process, a residual porosity of about 5% remains. During the pyrolysis, the matrix shrinks because of an increase in density. Volatile compounds evaporate, leading to the formation of porosity. The porosity is present as a network over the entire material which leads to some limitations in oxidation resistance. Furthermore, PIP needs very long processing times causing high production costs. The infiltration and pyrolysis steps have to be repeated up to eight times [3,13,19].

The LSI process, on the other hand, is a fast process consisting of only three manufacturing steps. The processing costs are therefore lower compared to PIP. LSI process leads to a very dense and oxidation resistant material. But composites manufactured via LSI contain a certain amount of unreacted carbon and excessive silicon which should be avoided. To protect the SiC fibers from the aggressive silicon melt, a complex and expensive fiber coating system has to be applied by means of chemical vapor deposition (CVD). The fracture strain is lower than with PIP material [8,21].

Therefore, we asked ourselves, whether it is possible to combine the two processes and profit from the advantages of both. The combined process can be beneficial compared to the individual processes in certain aspects: the densification of the PIP matrix and the reduction of unreacted carbon in the LSI process, for example. This work describes two approaches to establish a hybrid manufacturing process of PIP and RMI, specifically LSI. For the matrix construction, a reduced number of PIP cycles is followed by an additional liquid silicon infiltration process. One approach uses a polysilazane resin as PIP matrix precursor, another one is polycarbosilane based. Starting point for the PIP process was a CVD coated fiber preform consisting of layered Hi-Nicalon S woven fabrics.

2. Material and methods

The new hybrid manufacturing process for SiC/SiC composites is shown in Fig. 1 and is a combination of two stand-alone CMC manufacturing processes. Starting with woven fiber preforms, a CVD fiber coating system was applied to protect the fibers from the aggressive silicon melt. A reduced number of polymer infiltration and pyrolysis (PIP) cycles using polysilazanes or polycarbosilanes as preceramic polymers was performed. Big interbundle voids were thereby filled with a polymer derived SiC(N) matrix. As polysilazane PSZ20 (Clariant SE, Germany) was used. PSZ20 contains nitrogen and forms a SiCN ceramic matrix after high temperature heat treatment [19]. Polycarbosilane SMP-10 (Starfire Systems Inc., USA) is a nitrogen-free polymeric precursor, which forms stoichiometric SiC [22]. For the final liquid silicon infiltration (LSI) step, a novolac-type phenolic resin (Hexion GmbH, Germany) was infiltrated into the PIP material. After pyrolysis the porous carbon/SiC(N) matrix was infiltrated with liquid silicon or silicon alloy forming SiC and densifying the composite.

Stand-alone LSI process has 80% shorter processing times compared to PIP. By reducing the total number of PIP cycles to three in the hybrid process, the overall processing time was 45% shorter compared to stand-alone PIP process. It was even 55% shorter with only two PIP cycles. The hybrid manufacturing process offers great potential to reduce the production cost of PIP process.

2.1. Characterization of the matrix precursor

The crystallization behavior of SMP-10 and PSZ20 in argon atmosphere was investigated. Cured precursor materials were pyrolyzed in argon atmosphere for 10 h at different pyrolysis temperatures from 900 °C to 1500 °C varied in 100 K steps. All samples were weighed after curing and after pyrolysis to determine the temperature dependent mass yield. The bulk density was determined using Archimedes method according to DIN EN 623-2. In order to eliminate the effect of open porosity, the skeletal density was calculated in addition to the bulk density as

shown in equations (1) and (2). In the following, the skeletal density is referred to as density. The volume yield was calculated according to equation (3). Finally, crystallization was determined by the means of XRD measurements from 2θ = 10–90° with a step size of 0.01° and a scanning time per step of 10 s (D8 Advance, Bruker Corporation, Germany).

$$\rho_{bulk} = \frac{m_{dry}}{m_{wet} - m_{under\ water}} * \rho_{water} \quad (1)$$

$$\rho_{skeletal} = \frac{m_{dry}}{m_{dry} - m_{wet}} * \rho_{water} \quad (2)$$

$$volume\ yield = mass\ yield * \frac{\rho_{cured}}{\rho_{pyrolized}} \quad (3)$$

2.2. Manufacturing and characterization of the composites

Starting point for this investigation of the combined hybrid process PIP and LSI were findings of Schukraft and Koch from experimental studies performed at DLR Stuttgart [23]: SiC fiber reinforced composites were manufactured using Tyranno SA3 Fibers (UBE Industries, LTD., Japan). Several cycles of polymer infiltration and pyrolysis with the polysilazane PSZ20 were performed. After the infiltration of these composites with phenolic resin followed by pyrolysis in nitrogen atmosphere, harsh amounts of Si_3N_4 whiskers were detected. It is believed that the whiskers hindered the final infiltration of liquid silicon into the material. As critical factors for whisker formation, the influence of nitrogen, oxygen impurities and water contact were found. To establish the idea of a hybrid manufacturing process consisting of PIP and LSI processes, the first aim of this work was to eliminate the formation of whiskers in order to enable the final infiltration with silicon melt in general. Therefore, curing and pyrolysis was carried out in an argon atmosphere instead of nitrogen to prevent whisker formation. A silicon boron alloy with 8 at% boron was used for the liquid silicon infiltration to reduce siliconization temperature and decrease the aggressiveness of the melt [24]. Furthermore, any contact of the samples to oxygen or water was avoided to eliminate their influence on whisker formation. Therefore, the samples were stored in a glovebox in argon atmosphere, the tempering step in air was eliminated and porosity and density measurements using water were omitted.

In this work, SiC fiber reinforced composites were manufactured using polymer infiltration and pyrolysis followed by liquid silicon infiltration as shown in Fig. 1. Five layers of woven (8 harness satin) Hi-Nicalon S fabric (NGS Advanced Fibers Co., Ltd., Japan) were stacked and a fiber coating system was applied to the whole stack by chemical vapor deposition (CVD). A three-layer coating consisting of BN, SiC and pyrolytic carbon was chosen (Archer Technicoat Ltd, United Kingdom). The build-up of the coating is described elsewhere [21]. The size of the coated fiber fabric preform was 200 × 200 mm^2 while the thickness was 2 mm which resulted in a fiber volume content of 29.2%. Then, one to five cycles of PIP were performed. As matrix precursor either polycarbosilane SMP-10 (Starfire Systems Inc, USA) or polysilazane PSZ20 (Clariant SE, Germany) was used. For the infiltration of the preceramic polymer, resin transfer molding (RTM) was used. Before the infiltration, 1 wt% dicumyl peroxide (Alfa Aesar, Germany) was dissolved in 1 wt% toluene and was added to the polymeric precursors as a catalyst. Curing was performed inside the RTM mould at 260 °C for 5.5 h at a pressure of 15–20 bar for SMP-10 and PSZ20. The pyrolysis was perfomed at a constant gas flow of 800 l/h in argon atmosphere at atmospheric pressure at 1300 °C (HT 1800 GT, Linn High Therm GmbH, Germany). After the last PIP cycle a novolac-type phenolic carbon precursor with the internal designation MF88 (Hexion GmbH, Germany) was infiltrated via RTM and cured at 150 °C at a pressure of 15 bar in argon atmosphere. The final pyrolysis at 1400–1450 °C in a constant argon gas flow of 1200 l/h at atmospheric pressure formed a porous carbon matrix. The following infiltration with liquid silicon converted the carbon matrix to silicon carbide. A silicon boron alloy in eutectic composition (8 at% boron) was used for melt infiltration in reduced atmosphere (<2 mbar absolute pressure). The addition of boron to the silicon melt reduces the melting point, allowing the siliconization temperature to be lowered from 1450 °C to 1400 °C compared to pure silicon [25]. The final pyrolysis as well as the following liquid silicon infiltration was carried out in a high temperature graphite furnace (FCT Anlagenbau GmbH, Germany).

Table 1
Overview of the manufactured composite variants.

	polymer precursors	# of PIP cycles	gas atmosphere	alloy
Starting point [23]	PSZ20 + MF88	3; 6	nitrogen	pure Si
Approach #1	PSZ20 + MF88	1 … 5	argon	Si92B8
Approach #2	SMP-10 + MF88	1 … 5	argon	Si92B8
Approach #3	SMP-10 + MF88	2	argon	Si92B8

In the first approach (#1), polysilazane PSZ20 was used, while the processing was carried out in argon atmosphere as described above. The number of preliminary PIP cycles was varied from one to five. The second approach (#2) was comparable to the first one but the nitrogen-free precursor polycarbosilane SMP-10 was used. In the third approach (#3), a whole plate with the dimensions of 90 × 200 × 2 mm^3 was manufactured with two preliminary cycles of PIP using polycarbosilane SMP-10. An overview of the different composite variants manufactured is given in Table 1. For mechanical characterization, eight bending specimens and four tensile specimens of the manufactured plate in approach #3 with the dimensions of 90 × 10 × 2 mm^3 were tested. Three of the bending specimens were oxidized at 1200 °C for 100 h at a constant air flow of 600 l/h at atmospheric pressure before mechanical testing (HT 1800 GT, Linn High Therm GmbH, Germany). Strain rates were measured using strain gauges. A displacement-controlled test method with a rate of 1 mm/min was chosen. The length/thickness ratio used for four-point bending testing was 20. To measure the proportional limit stress, a method was chosen in which a strain displacement of 0.005% was taken parallel to the slope of the linear section of the stress-strain curve. Its intersection with the stress-strain curve of the material was determined. The stress value at this intersection is called the proportional limit stress (PLS). It is the measure at which the inelastic behavior of the material begins. Microstructure of the composites was examined using EDS and SEM at a voltage of 10 kV and magnifications of 180 x, 250 x, 1 kx, 3 kx and 7.5 kx (Zeiss Ultra Plus, Carl Zeiss Microscopy GmbH, Germany). For fractured surfaces the SE2 detector was used, for polished ones the AsB detector.

For monitoring the development of the matrix formation during the hybrid manufacturing process, one sample with the size of 90 × 10 × 2 mm was prepared for µCT measurements. After each processing step µCT scans were performed at the exact same position. The µCT scans were conducted using a high resolution µCT-System (nanotom, GE Sensing & Inspection Technologies GmbH, Germany) consisting of a microfocus X-ray tube with a maximum accelerating voltage of 180 kV and a 12-bit flat panel detector (active area 2348 × 2348 pixels at 50 µm per pixel). The µCT scans were performed with the X-ray parameters 80 kV(voltage) and 180 µA (current) at an exposure time of 800 ms. A voxel size of 3.5 µm could be achieved. The so acquired 2D X-ray images were reconstructed with a special reconstruction algorithm known as Filtered Back Projection. The µCT data were visualized and analyzed with the software package VGStudioMax 3.2 (Volume Graphics GmbH, Germany).

3. Results

3.1. Characterization of the matrix precursor

Fig. 2 a and c show the diffractograms of SMP-10 and PSZ20 samples pyrolyzed for 10 h at temperatures from 1100 °C to 1500 °C in argon

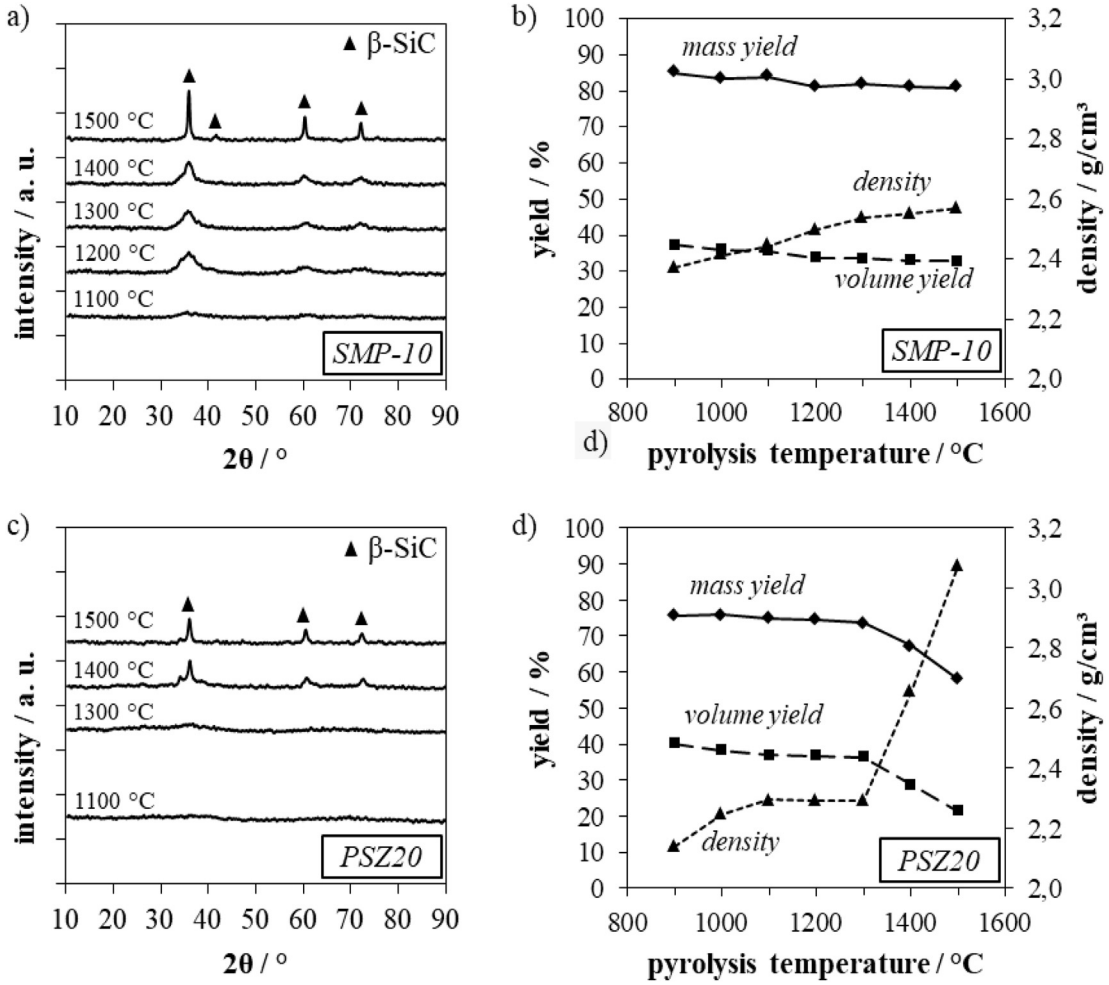

Fig. 2. Characterization of the polymeric precursors SMP-10 and PSZ20. Pyrolysis of cured sample material was carried out in argon atmosphere for 10 h. Crystallization of SMP-10 and PSZ20 (a) and (c). Mass yield, density and volume yield of SMP-10 and PSZ20 (b) and (d).

Table 2
Measured densities, mass yields and volume yields of SMP-10 and PSZ20. The yields are based on the density of the cured precursor.

Temperature /°C	Density SMP-10 /g/cm^3	Mass yield SMP-10 /%	Vol. yield SMP-10 /%	Density PSZ20 /g/cm^3	Mass yield PSZ20 /%	Vol. yield PSZ20 /%
As received	1.00	–	–	1.02	–	–
Cured	1.04	–	–	1.13	–	–
900	2.37	85.16	37.33	2.14	75.79	40.02
1000	2.41	83.44	35.93	2.25	75.86	38.15
1100	2.45	83.90	35.65	2.30	75.02	36.94
1200	2.50	81.12	33.74	2.29	74.64	36.80
1300	2.54	81.98	33.56	2.29	73.71	36.34
1400	2.55	81.07	33.03	2.66	67.23	28.60
1500	2.57	81.02	32.78	3.08	58.12	21.36

atmosphere. With increasing temperature, the ceramics convert from fully X-ray amorphous to a pronounced crystalline structure. The conversion of SMP-10 derived amorphous SiC to crystalline β-SiC was already detected at 1200 °C, evolving at 1500 °C into sharp X-ray reflexes. Crystallization of the polysilazane derived SiCN to β-SiC is only about to start at temperatures 200 K higher compared to SMP-10. Surprisingly, no X-ray reflexes associated with Si_3N_4 could be observed. The higher the pyrolysis temperature, the sharper the X-ray reflexes become and crystallinity of the SiC(N) ceramics increases. Simultanously, densities are expected to increase too. Fig. 2 b and d show the temperature dependent change of density as well as mass and volume yield. The corresponding values are summarized in Table 2. Mass and volume yield values are based on cured precursor material. The density of SMP-10 pyrolyzed at 900 °C was determined to be 2.37 g/cm^3 and increases with an almost constant rate to 2.57 g/cm^3 for the maximum chosen temperature of 1500 °C. Meanwhile, volume yield drops slightly from 37.33% to 33.03%. A lower density of 2.14 g/cm^3 at a pyrolysis temperature of 900 °C was analyzed for PSZ20, but a much higher one of 3.08 g/cm^3 at 1500 °C. The density increases considerably faster, starting from 1300 °C. However, the volume yield drops by almost 20% to a final value of 21.36%, which is about 30% less compared to SMP-10.

3.2. Characterization of the composites

3.2.1. Preliminary studies

During the manufacturing of ceramic composites via the hybrid manufacturing process using polysilazane PSZ20 as described in chapter 2.2, formation of Si_3N_4 whiskers occurred in the work of Schukraft and Koch. The whiskers were identified using X-ray diffraction method and SEM analysis (Fig. 3 a, b) [23]. Whiskers were mainly formed during the last pyrolysis of phenolic resin MF88 in nitrogen atmosphere. Whisker formation has significantly been reduced by avoiding the contact of samples with nitrogen, water and oxygen in approach #1 of this work. Only small amounts of whiskers were formed mainly at the edges and corners of the samples (Fig. 3 c). By usage of the nitrogen-free precursor SMP-10 in approach #2 whisker formation could finally be eliminated as seen in

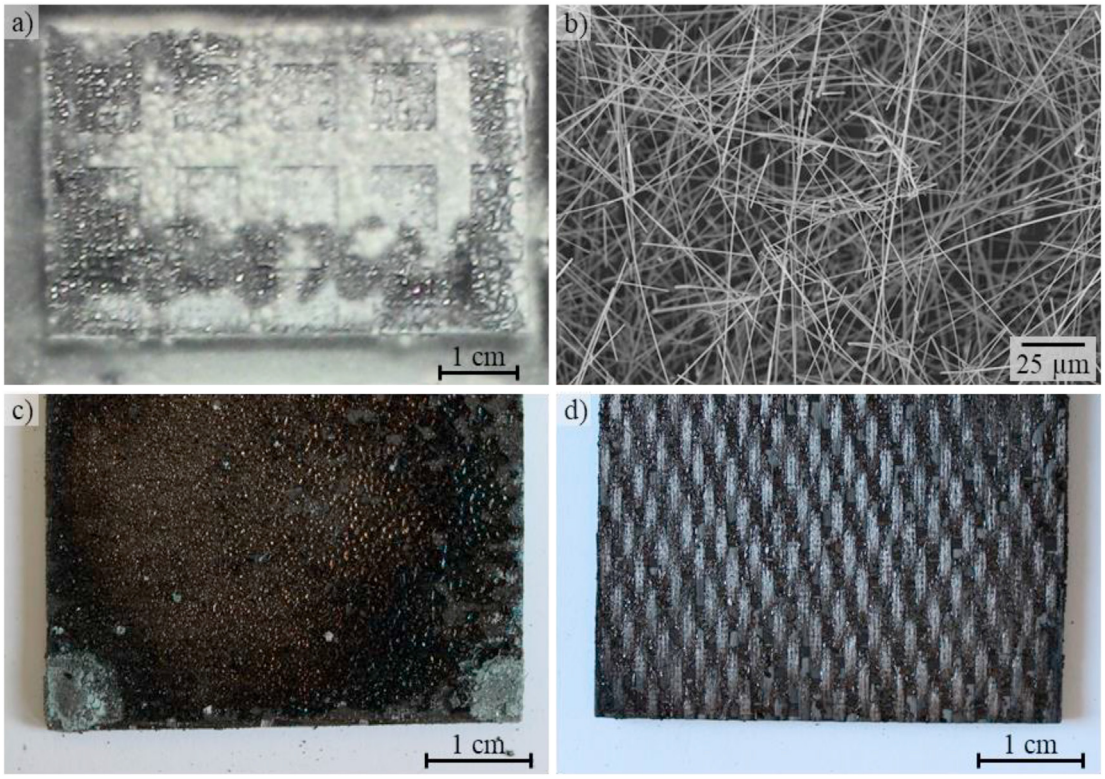

Fig. 3. Whisker formation after pyrolysis of phenolic resin in nitrogen atmosphere (a). SEM image of Si_3N_4 whiskers (identified by XRD) (b) [23]. Reduced whisker formation when pyrolyzed in Ar instead of N_2, water and oxygen contact was avoided, too (approach #1) (c). No whisker formation was observed when polycarbosilane precursor SMP-10 was used in approach #2 (d).

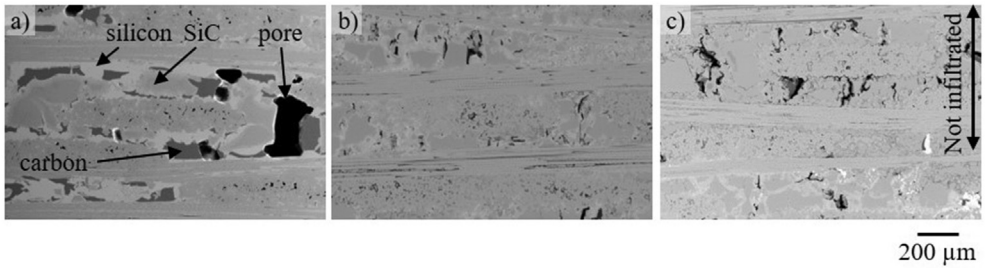

Fig. 4. Hybrid CMC after siliconization with (a) one polymer infiltration and pyrolysis cycle, (b) three cyles and (c) five cycles (approach #2).

Fig. 3 d. Therfore, it was decided that polycarbosilane SMP-10 is more suited for hybrid manufacturing process compared to polysilazane PSZ20.

The influence of different numbers of preliminary PIP cylces before the LSI step was examined. Composites with one, three and five polymer infiltration and pyrolysis cycles with SMP-10 followed by LSI process were manufactured (approach #2). A silicon-boron alloy in eutectic composition was used for melt infiltration. The open porosity of the siliconized samples measured using Archimedes method were 1.4% for the samples with one preliminary PIP cycle, 8.8% with three cycles and 6.9% with five cycles. The quality of the silicon infiltration was further examined using SEM analysis of the infiltrated samples (see Fig. 4). After one cycle, some residual carbon blocks and large pores remained, probably closed porosity. After three cycles no carbon blocks could be seen, but a few smaller pores. Despite the lower open porosity, it was found that after five cycles the silicon could not be infiltrated through the entire thickness of the sample. Silicon could only be detected a few hundred micrometers from the surface. The rest of the sample was not infiltrated as indicated in Fig. 4 c.

The need for a protective fiber coating system was assessed. A few samples were manufactured without additional fiber coating. In these composites, the SiC fibers were destroyed in contact with the silicon melt. It was found that even five cycles of PIP were not enough to protect the fibers from silicon attack. This assessment leads to the conclusion that, a protective CVD fiber coating system is required for the hybrid manufacturing process.

3.2.2. SiC/SiC composite plate

For the manufacturing of a larger SiC/SiC composite plate with dimensions of 200 × 90 × 2 mm^3 in approach #3, it was decided to perform two cycles of PIP before the final LSI step. The aim was to use a hybrid process which is as short as possible but reasonable. The plate was siliconized in standing position inside a boron nitride coated graphite crucible. The whole surface was covered with silicon after the siliconization process. One sample of the plate with dimensions 90 × 10 × 2 mm^3 was cut off in SiC-fiber reinforced polymer state. This sample was used for µCT measurements. µCT scans were conducted at the exact same position after each step of the hybrid process: 1.) after two polymer infiltration and pyrolysis cycles 2.) after infiltration and pyrolysis of the phenolic resin 3.) after siliconization. Images of the µCT scans are shown in Fig. 5. Despite the dense-looking surface of the plate, µCT measurements revealed

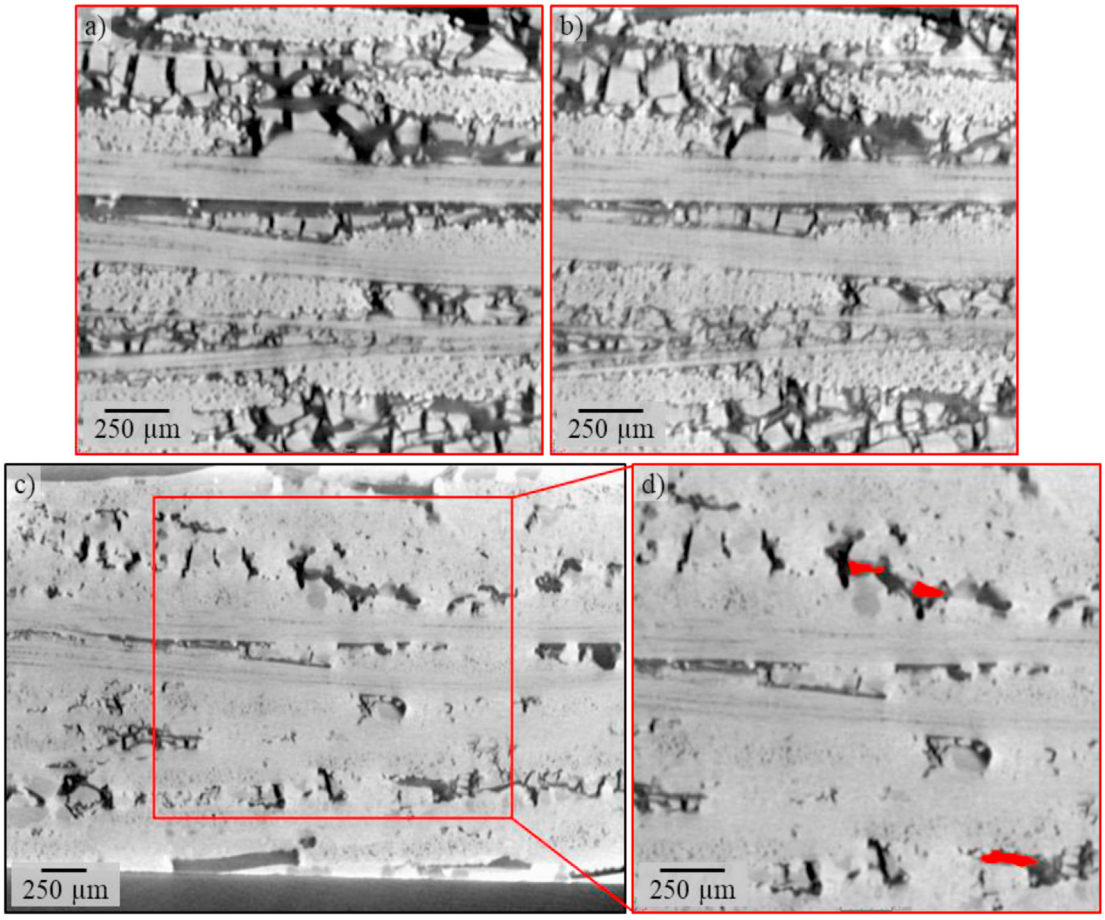

Fig. 5. µCT scans at the same area of one sample of (a) after 2 cycles of polymer infiltration and pyrolysis, (b) after the infiltration of phenolic resin and pyrolysis (c) and (d) after melt infiltration with liquid silicon. Residual carbon after siliconization is highlighted in red. (For interpretation of the references to colour in this figure legend, the reader is referred to the Web version of this article.)

remaining porosity in the inner part of the plate as seen in Fig. 5 d. The spatial and contrast resolution were not high enough for an automated determination of the pore and carbon content. Therefore, pores and residual carbon could not be separated based on user-independent automatic algorithms. Some excess carbon was highlighted in red colour manually in the image. Therefore, open porosity after siliconization was determined for four samples of the plate via Archimedes method to 11.4 ± 0.9%. Carbon content after siliconization could not be determined from µCT scans; therefore, SEM images in different parts of the samples were used to determine the residual carbon content of the composite via grey value analysis. In total, 10 images at a magnification of 100 were used. The residual carbon content is 3.1 ± 0.5%.

The microstructure of the composite was examined using SEM in backscatter electron mode (Fig. 6 a-c). The microstructure is composed of the matrix and SiC fibers with a BN and SiC CVD fiber coating. The matrix consists of SiC resulting from polymer infiltration and pyrolysis, free silicon and recrystallized SiC which was formed during liquid silicon infiltration. Elemental analysis was performed on the different SiC components of the matrix using energy dispersive x-ray spectroscopy. For each area [1], [2], [3] and [4], at least five single EDS spots were analyzed. The mean values for silicon, carbon and oxygen contents are shown in the table in Fig. 6. The composition of the recrystallized SiC is comparable for the areas [3] and [4] even though its structure seems to be foamy in area [3]. SiC resulting from PIP [1] has an additional oxygen content of 5%. Also, the thin layer [2] around the SiC_{PIP} matrix block shows 4% oxygen. However, the carbon content in this layer is lower and the silicon content is higher than in the inner core of the SiC_{PIP} block [1]. The formation of the described layer cannot be explained yet and is part of further investigation. It is assumed that the outer part of the polymer derived silicon carbide blocks was attacked in contact with free silicon.

Scanning electron micrographs showed as well that the fiber coating system remained only partly intact, depending on the composition of the surrounding microstructure. In contact with a large amount of silicon strong attack of the coatings and fibers was shown (Fig. 6 c). In areas with a larger SiC matrix proportion the coatings and fibers remained intact (Fig. 6 b). The stability of the coating is also dependent on their local arrangement in the microstructure. At the edge of the fiber bundles the fibers and coatings are more likely to degrade than in the center.

For mechanical characterization, five four-point bending specimens and four tensile specimens of the manufactured plate in approach #3 were tested in as manufactured state. Three bending specimens were oxidized at 1200 °C for 100 h in air before testing. Representative stress-strain curves are plotted in Fig. 7. The mean values of all samples and their standard deviations are shown in Fig. 8, all values are summarized in Table 3. Bending strength as manufactured was 433 MPa. After oxidation, bending strength reduced by 42% – 250 MPa. Strain to failure reduced by 51% from 0.6 to 0.29%. Surprisingly, the proportional limit stress remained almost stable after oxidation; it decreased only slightly from 186 to 181 MPa. Ultimate tensile strength was 189 MPa, strain to failure was 0.18%. Both values were significantly lower compared to the bending tests. The bending/tensile strength ratio was 2.3. Proportional limit stress determined from tensile tests was 105 MPa. SEM images of fractured surfaces are shown in Fig. 9. Very good fiber pull out was observed in the bending samples after testing in as manufactured state. The pull-out length was around 50–150 µm. The pull-out length of the tensile specimens was significantly shorter. Fiber

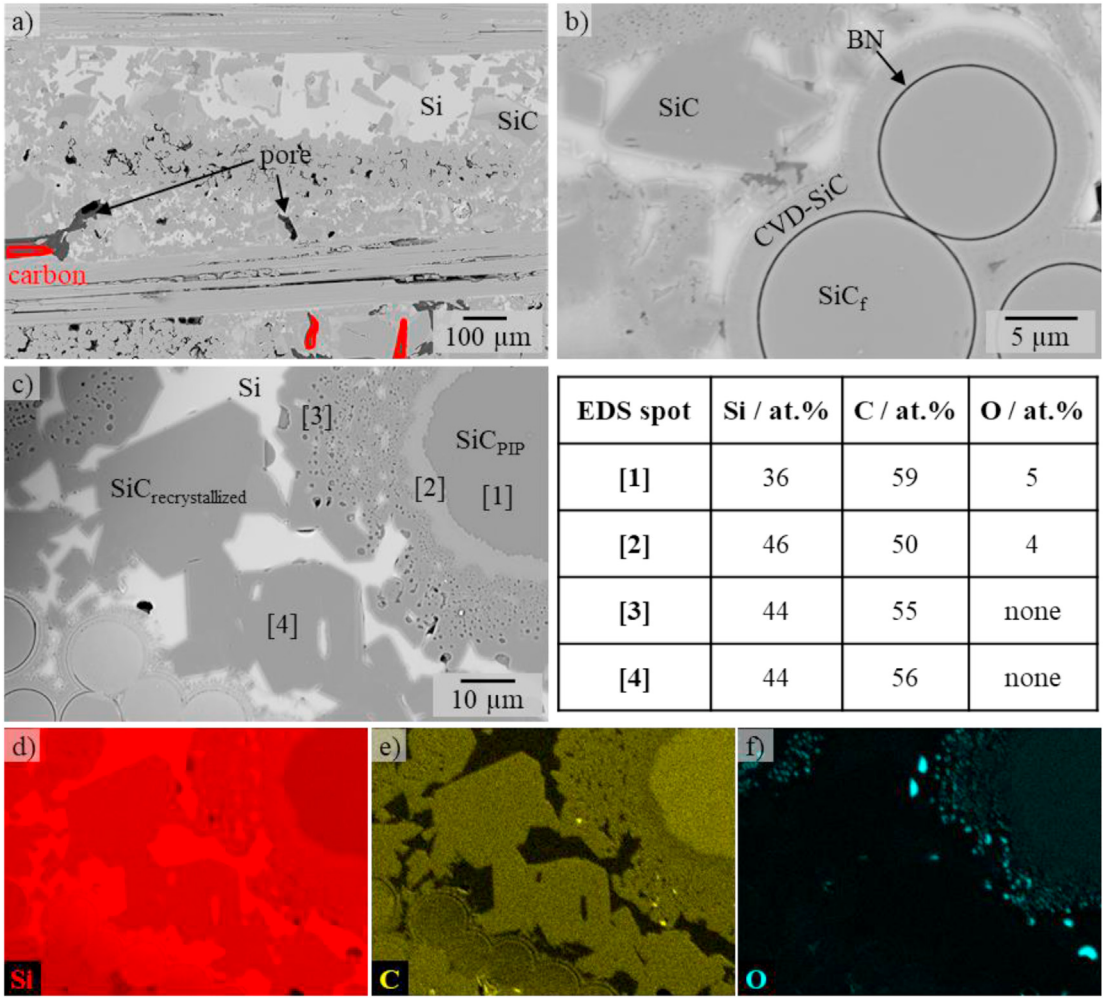

EDS spot	Si / at.%	C / at.%	O / at.%
[1]	36	59	5
[2]	46	50	4
[3]	44	55	none
[4]	44	56	none

Fig. 6. Microstructural analysis of the manufactured hybrid CMC in approach #3. (a) to (c) shows SEM images in backscatter electron mode. The microstructure components are labeled in the images. Element maps of the silicon (d), carbon (e) and oxygen (f) distribution. Elemental compositions were measured in the areas [1], [2], [3] and [4]. The mean values are given in the table. (For interpretation of the references to colour in this figure legend, the reader is referred to the Web version of this article.)

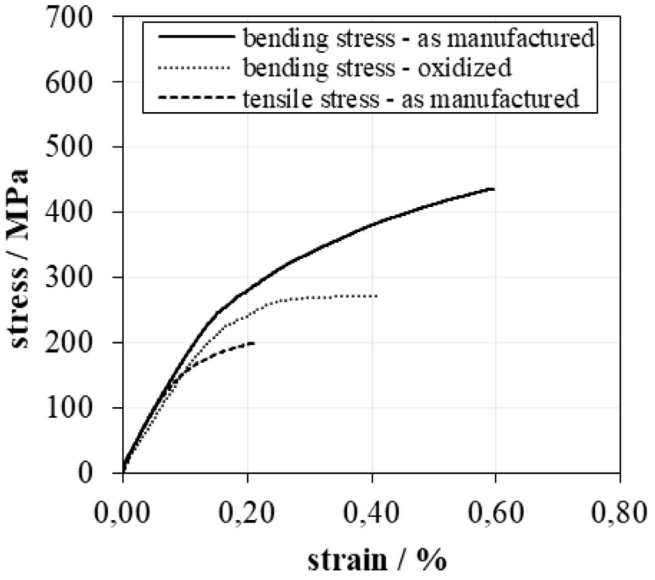

Fig. 7. Representative stress-strain curves of the manufactured hybrid composite in approach #3.

pull out length was also shorter with bending specimens tested after oxidation treatment.

4. Discussion

Since the pyrolysis atmosphere was changed, the crystallization behavior of the preceramic polymers SMP-10 and PSZ20 in argon atmosphere was investigated (see Fig. 2 in chapter 3.1). Mainzer et al. characterized the crystallization behavior of polysilazane in nitrogen atmosphere in detail [19]. Compared to the results in this work, the crystallization of polysilazane in nitrogen atmosphere starts 200 K later at 1600 °C. The amorphous SiCN matrix crystallizes to β-SiC and Si_3N_4 in nitrogen atmosphere. The decomposition of the SiCN ceramic due to the carbothermal reduction at higher temperatures follows equation (4) [26]. In argon atmosphere no crystallization of Si_3N_4 could be detected because gaseous nitrogen is released from the system. As a result, the reaction equilibrium is shifted to the side of the products and formation of crystallized Si_3N_4 is suppressed: only SiC is formed. The lower crystallization temperature for PSZ20 in argon atmosphere can be explained by thermodynamical calculations of Seifert and Markel [26,27]. The decomposition temperature of the Si-C-N system is dependent on the partial pressure of nitrogen. Decomposition temperature decreases from 1484 °C at 1 bar nitrogen atmosphere to 1312 °C at 0.1 bar. This is in good agreement with what was identified as start temperature of

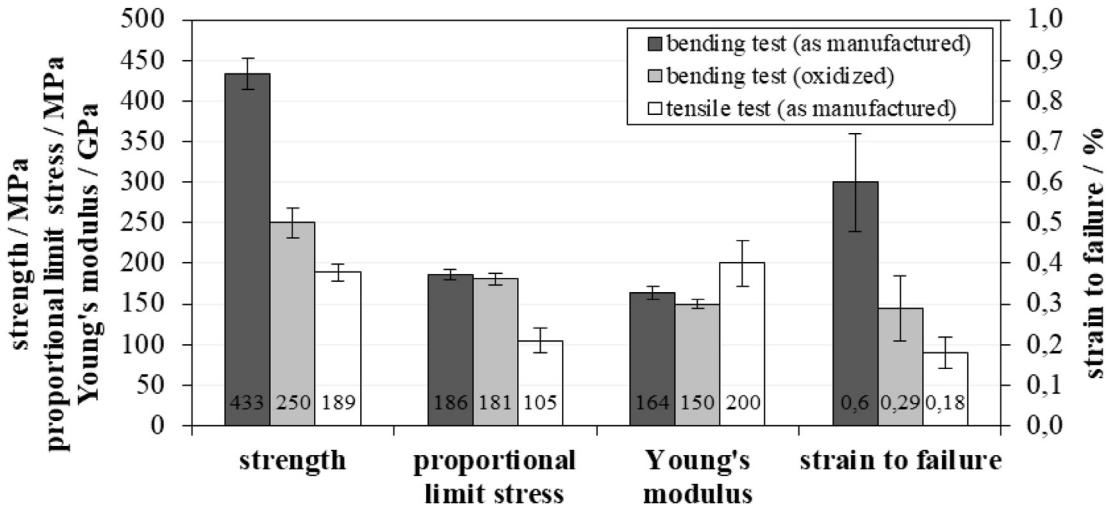

Fig. 8. Comparison of the mechanical properties of the hybrid composite manufactured in approach #3 in four-point bending testing before and after oxidation, as well as in tensile testing.

Table 3
Mechanical properties of the composite manufactured in approach #3.

	as manufactured	oxidized (1200 °C, 100 h, air)
σ_{4PB} /MPa	433 ± 19	250 ± 18
PLS_{4PB} /MPa	186 ± 6	181 ± 7
E_{4PB} /GPa	164 ± 8	150 ± 6
ε_{4PB} /%	0.60 ± 0.12	0.29 ± 0.08
$\sigma_{tensile}$ /MPa	189 ± 10	–
$PLS_{tensile}$ /MPa	105 ± 15	–
$E_{tensile}$ /GPa	200 ± 28	–
$\varepsilon_{tensile}$ /%	0.18 ± 0.04	–

crystallization in argon atmosphere for PSZ20. Since the pyrolysis of PSZ20 is carried out at temperatures below its decomposition temperature, the SiCN matrix will remain amorphous. The use of argon atmosphere instead of nitrogen will not affect the amorphous structure in this case.

$$Si_3N_{4(s)} + 3C_{(s)} \rightarrow 3SiC_{(s)} + 2N_{2(g)} \quad (4)$$

$$3\,SiO_{(g)} + 3\,C_{(s)} + 2\,N_{2\,(g)} \rightarrow Si_3N_{4\,(s)} + 3\,CO_{(g)} \quad (5)$$

During the hybrid manufacturing process for SiC/SiC composites, formation of Si_3N_4 whiskers occurred when polysilazane was used as preceramic polymer (see Fig. 3 a, b in chapter 3.2.1). Curing and pyrolysis were performed in nitrogen atmosphere [23]. The formation of Si_3N_4 whiskers is based on equation (5) [28]. In this case, whiskers do not act as a desirable strengthening phase. Si_3N_4 whiskers hinder the final silicon infiltration due to the high contact angle between Si/Si_3N_4 of 49° and their high surface area. The final contact angle in the desired system which consists of liquid silicon and amorphous carbon would be only 36° [29]. Furthermore, whiskers are hazardous for the operator of the manufacturing facilities. Gaseous SiO reacts with solid C and gaseous N_2 forming Si_3N_4 whiskers and CO gas. To prevent this reaction, the presence of nitrogen and SiO gas in the following manufacturing processes was avoided. Therefore, curing and pyrolysis atmospheres were switched from nitrogen to argon. SiO formation can occur due to oxygen contamination. Oxygen can be implemented into the SiC(N) matrix by tempering the cured precursors in oxygen atmosphere, by storing the samples in air, or due to contact with water. Consequently, all activities where oxygen contamination can take place were avoided.

The whisker formation could be significantly reduced by using argon atmosphere and avoiding contact with oxygen or water. Only small amounts of whiskers were formed at the edges and corners of the samples manufactured in approach #1 (see Fig. 3 c in chapter 3.2.1). During the decomposition of the SiCN matrix, nitrogen gas emerges according to equation (4). As a result of which, whisker formation could not be prevented completely. By the use of nitrogen-free precursor SMP-10 in approach #2, whisker formation could finally be eliminated. Therfore, it was found that polycarbosilane SMP-10 is more suited for the hybrid manufacturing process.

The influence of different numbers of preliminary PIP cylces with SMP-10 before the LSI step was examined in approach #2. By varying the amount of PIP cycles, it could be found that one to three PIP cycles before the LSI step was more than sufficient as seen in Fig. 4 in chapter 3.2.1. When more cycles were used, the composite was already too dense and the silicon could not be infiltrated through the entire thickness of the sample. With only one preliminary PIP cycle, some unreacted carbon was still remaining. In order to use a hybrid manufacturing process as short as possible but reasonable, it was decided to manufacture a larger SiC/SiC plate using two cycles of PIP before the final LSI step (approach #3). SEM analysis and μCT scans revealed a high amount of porosity in the inner

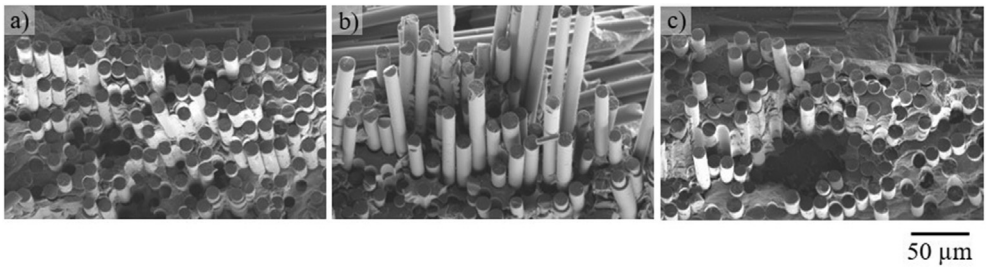

Fig. 9. Fracture surfaces of (a) tensile specimen (b) bending specimen and (c) bending specimen after oxidation at 1200 °C for 100 h.

Table 4
Comparison of different processing routes for SiC/SiC at DLR.

	PIP	LSI	Hybrid PIP + LSI
Processing time compared to PIP		80% less	55% less
Residual carbon	None	10.3%	3.1%
Need of fiber coating	No	Yes	Yes
Porosity	5%	<3%	11.4%

part of this plate. Only the outer layers were fully siliconized. The reason why liquid silicon did not fully infiltrate the pore structure of the composite could not be explained and is part of ongoing research. A possible explanation is that the growth of recrystallized SiC closed the accesses to the pore channels blocking further infiltration of silicon. The optimization of the siliconization conditions has to be improved and is part of future research. Fully dense composites with porosity values below 3% comparable to pure LSI material are aimed. Very positive and promising is the fact that the carbon content of the hybrid material was successfully reduced by 70% compared to LSI material. Large interbundle voids were filled with SiC during PIP process as expected.

Mechanical testing revealed a high discrepancy between tensile and bending strength of factor 2.3. Differing values for tensile and bending strength were reported in literature before. The higher bending strength was explained by the different behavior of brittle CMCs in compression and tension caused by matrix cracking. The linear compression behavior supports the tensile side of the bending specimen which shows a non-linear behavior. Therefore, the neutral axis is shifted to the tensile side followed by a decrease of stress on the tensile side [30–32]. Hild et al. described this phenomenon with Nicalon fibers. Hofmann et al. found a bending/tensile ratio of approximately 1.7 for C/C-SiC material manufactured via LSI process. But this approach can only partly explain the high factor of 2.3. Additionally, there might have been some stress overloads due to the fact that tensile specimens without a reduced gauge width compared to grip width were used. Furthermore, the size effect of a Weibull distribution of flaws is higher in tensile testing compared to bending [33].

After oxidation in air at 1200 °C and 100 h, the bending strength decreased by 42% and strain to failure by 51%. Correspondingly, a shorter fiber pull out length was observed in oxidized bending specimens. This is an indication of higher frictional stresses between fiber and matrix after debonding in oxidized state. However, it is promising that the proportional limit stress remained almost the same and only decreased by 3%. In former work by Klatt et al. the bending strength of pure PIP material decreased by 70% and the strain to failure by even 81% at oxidation at lower temperatures of 1100 °C and only 20 h [34]. Improved PIP material by Mainzer showed a decrease of bending strength of 54% after oxidation at 1200 °C for 10 h [35]. Chai et al. measured a comparable strength decrease of 51% for PIP SiC/SiC material oxidized for 1 h at 1200 °C [36]. In this work, it can be shown that the oxidation behavior of pure PIP material was improved by final siliconization even though the porosity was rather high. It is expected that oxidation behavior could be further improved by a more complete silicon infiltration and a better densification of the matrix. Nevertheless, the oxidation behavior still needs to be improved considerably. GE's benchmark material HiPerComp (Prepreg), for example, shows almost no decrease of the ultimate strength after exposure in air at 1200 °C for up to 1000 h [8]. However, GE is using a multifold external oxidation protection coating which will be needed and tested in future development programs.

5. Conclusions

A new hybrid manufacturing process for SiC/SiC CMCs consisting of PIP and LSI processes was developed. Whisker formation was completely eliminated by using polycarbosilanes instead of polysilazanes for PIP. Curing and pyrolysis was performed in argon instead of nitrogen atmosphere. It must be noted that crystallization of polysilazane starts 200 K earlier in argon compared to nitrogen. After several preliminary tests, a larger plate was successfully produced. The microstructure, mechanical properties and oxidation behavior were investigated.

One to three PIP cycles before the final LSI step were sufficient; with more infiltrations the matrix was already too dense for melt infiltration. By using only two PIP cycles the overall processing time could be reduced by 55% compared to stand-alone PIP process (Table 4). As weak interphase and to protect the fibers from the aggressive silicon melt, a CVD fiber coating system is required. By filling large interbundle voids with PIP-derived SiC matrix material, the residual carbon content could be reduced by 70% compared to the stand-alone LSI process. Siliconization of PIP-derived matrix is beneficial for the oxidation resistance of the composite.

Nevertheless, a completely dense matrix could not be achieved so far. This has to be improved in future work to establish the new hybrid process as a real alternative to the stand-alone processes.

Declaration of competing interest

The authors declare that they have no known competing financial interests or personal relationships that could have appeared to influence the work reported in this paper.

Acknowledgements

Financial support of the CMC_TraTurb project (03XP0169E) by the Bundesministerium für Bildung und Forschung (Germany) is gratefully acknowledged. The authors thank Daniel Cepli for mechanical testing, Matthias Scheiffele for RTM infiltrations and Dr. Yuan Shi for his helpful advice.

References

[1] J. DiCarlo, H.-M. Yun, G. Morscher, R. Bhatt, SiC/SiC composites for 1200°C and above, in: N. Bansal (Ed.), Handbook of Ceramic Composites, Springer, 2005, pp. 77–98.
[2] Flightpath EuropeanCommission, 2050 - Europe's Vision for Aviation: Maintaining Global Leadership and Serving Society's Needs, Publications Office of the EU, 2012.
[3] D. Kopeliovich, Advances in the manufacture of ceramic matrix composites using infiltration techniques, in: I. Low (Ed.), Advances in Ceramic Matrix Composites, Elsevier, 2014, pp. 79–108.
[4] A. Kohyama, CMC for nuclear applications, in: W. Krenkel (Ed.), Ceramic Matrix Composites, Wiley, 2008.
[5] Y. Katoh, L.L. Snead, C.H. Henager, A. Hasegawa, A. Kohyama, B. Riccardi, H. Hegeman, Current status and critical issues for development of SiC composites for fusion applications, J. Nucl. Mater. 367–370 (2007) 659–671.
[6] C. Sauder, A. Brusson, J. Lamon, Influence of interface characteristics on the mechanical properties of hi-nicalon type-S or tyranno-SA3 fiber-reinforced SiC/SiC minicomposites, Int. J. Appl. Ceram. Technol. 7 (3) (2010) 291–303.
[7] J. Steibel, Ceramic matrix composites taking flight at GE Aviation, Am. Ceram. Soc. Bull. 98 (3) (2019) 32–36.
[8] G. Corman, K. Luthra, Silicon melt infiltrated ceramic composites (HiPerComp™), in: N. Bansal (Ed.), Handbook of Ceramic Composites, Springer, 2005, pp. 99–115.
[9] G. Gardiner, Aeroengine composites, part 1: the CMC invasion, in: Composites World, Gardner Business Media Inc., 2015, pp. 38–41.
[10] G. Motz, S. Schmidt, S. Beyer, The PIP-process: precursor properties and applications, in: W. Krenkel (Ed.), Ceramic Matrix Composites, Wiley, 2008, pp. 165–186.
[11] P. Colombo, G. Mera, R. Riedel, G.D. Sorarù, Polymer-derived ceramics: 40 Years of research and innovation in advanced ceramics, J. Am. Ceram. Soc. 93 (7) (2010) 1805–1837.
[12] G. Ziegler, I. Richter, D. Suttor, Fiber-reinforced composites with polymer-derived matrix: processing, matrix formation and properties, Compos. Appl. Sci. Manuf. 30 (4) (1999) 411–417.
[13] B. Mainzer, M. Frieß, R. Jemmali, D. Koch, Development of polyvinylsilazane-derived ceramic matrix composites based on Tyranno SA3 fibers, J. Ceram. Soc. Jpn. 124 (10) (2016) 1035–1041.
[14] A. Licciulli, F.D. Riccardis, A. Quirini, C.A. Nannetti, G. Filacchioni, L. Pilloni, S. Botti, A. Ortona, A. Cammarota, Preparation and Characterization of SiC/C/SiC Composites by Hybrid Wet/vapour Processing, Key Engineering Materials, Trans Tech Publ, 1997, pp. 279–286.
[15] A. Ortona, A. Donato, G. Filacchioni, U. De Angelis, A. La Barbera, C.A. Nannetti, B. Riccardi, J. Yeatman, SiC–SiCf CMC manufacturing by hybrid CVI–PIP techniques: process optimisation, Fusion Eng. Des. 51 (2000) 159–163.

[16] C.A. Nannetti, A. Ortona, D.A. de Pinto, B. Riccardi, Manufacturing SiC-Fiber-Reinforced SiC matrix composites by improved CVI/slurry infiltration/polymer impregnation and pyrolysis, J. Am. Ceram. Soc. 87 (7) (2004) 1205–1209.
[17] K. Suzuki, K. Nakano, S. Kume, T. Chou, Ceramic Matrix Composites I-Fabrication and Characterization of 3-D Carbon Fiber Reinforced SiC Matrix Composites via Slurry and Pulse-CVI Joint Process, Ceramic Engineering and Science Proceedings, American Ceramic Society, Columbus, Ohio, 1998, pp. 259–266.
[18] K. Schönfeld, H. Klemm, Interaction of fiber matrix bonding in SiC/SiC ceramic matrix composites, J. Eur. Ceram. Soc. 39 (13) (2019) 3557–3565.
[19] B. Mainzer, C. Lin, R. Jemmali, M. Frieß, R. Riedel, D. Koch, Characterization and application of a novel low viscosity polysilazane for the manufacture of C- and SiC-fiber reinforced SiCN ceramic matrix composites by PIP process, J. Eur. Ceram. Soc. 39 (2–3) (2019) 212–221.
[20] S. Hönig, F. Süß, N. Jain, R. Jemmali, T. Behrendt, B. Mainzer, D. Koch, Evaluation of preparation and combustion rig tests of an effusive cooled SiC/SiCN panel, Int. J. Appl. Ceram. Technol. 17 (4) (2020) 1562–1573.
[21] B. Mainzer, R. Jemmali, P. Watermeyer, K. Kelm, M. Frieß, D. Koch, Development of damage-tolerant ceramic matrix composites (SiC/SiC) using Si-BN/SiC/pyC fiber coatings and LSI processing, J. Ceram. Sci. Technol. 8 (1) (2017) 113–120.
[22] S. Kaur, R. Riedel, E. Ionescu, Pressureless fabrication of dense monolithic SiC ceramics from a polycarbosilane, J. Eur. Ceram. Soc. 34 (15) (2014) 3571–3578.
[23] J. Schukraft, D. Koch, Entwicklung und Charakterisierung von langfaserverstärkten SiC/SiC-Werkstoffen, Institute of Applied Materials - Ceramic Materials and Technologies, Karlsruhe Institute of Technology, 2019.
[24] B. Mainzer, K. Kelm, P. Watermeyer, M. Frieß, D. Koch, How to Tame the Aggressiveness of Liquid Silicon in the LSI Process, Key Engineering Materials, Trans Tech Publ, 2017, pp. 238–245.
[25] R. Olesinski, G. Abbaschian, The B— Si (boron-silicon) system, Bull. Alloy Phase Diagr. 5 (5) (1984) 478–484.
[26] H.J. Seifert, J. Peng, H.L. Lukas, F. Aldinger, Phase equilibria and thermal analysis of Si–C–N ceramics, J. Alloys Compd. 320 (2) (2001) 251–261.
[27] I.J. Markel, J. Glaser, M. Steinbrück, H.J. Seifert, Experimental and computational analysis of PSZ 10- and PSZ 20-derived Si-C-N ceramics, J. Eur. Ceram. Soc. 39 (2–3) (2019) 195–204.
[28] P.C. Silva, J.L. Figueirdo, Production of SiC and Si3N4 whiskers in C+SiO2 solid mixtures, Mater. Chem. Phys. 72 (3) (2001) 326–331.
[29] B. Drevet, N. Eustathopoulos, Wetting of ceramics by molten silicon and silicon alloys: a review, J. Mater. Sci. 47 (24) (2012) 8247–8260.
[30] S. Hofmann, B. Öztürk, D. Koch, H. Voggenreiter, Experimental and numerical evaluation of bending and tensile behaviour of carbon-fibre reinforced SiC, Compos. Appl. Sci. Manuf. 43 (11) (2012) 1877–1885.
[31] F. Hild, J.-M. Domergue, F.A. Leckie, A.E. Evans, Tensile and flexural ultimate strength of fiber-reinforced ceramic-matrix composites, Int. J. Solid Struct. 31 (7) (1994) 1035–1145.
[32] P.S. Steif, A. Trojnacki, Bend strength versus tensile strength of fiber-reinforced ceramics, J. Am. Ceram. Soc. 77 (1994) 221–229.
[33] V. Laws, The relationship between tensile and bending properties of non-linear composite materials, J. Mater. Sci. 17 (1982) 2919–2924.
[34] E. Klatt, A. Frass, M. Frieß, D. Koch, H. Voggenreiter, Mechanical and microstructural characterisation of SiC- and SiBNC-fibre reinforced CMCs manufactured via PIP method before and after exposure to air, J. Eur. Ceram. Soc. 32 (14) (2012) 3861–3874.
[35] B. Mainzer, Entwicklung von keramischen SiC/SiC-Verbundwerkstoffen mit Tyranno SA3 Fasern auf Basis des PIP- und LSI-Verfahrens, Karlsruhe Institute of Technology, 2019.
[36] Y. Chai, X. Zhou, H. Zhang, Effect of oxidation treatment on KD–II SiC fiber–reinforced SiC composites, Ceram. Int. 43 (13) (2017) 9934–9940.